Analysis of Pyrolysis Process for *Spirulina* and *Scenedesmus* Microalga in A Rotary Kiln and The Composition of Their Resultant Bio-Oils

Bothwell Nyoni[1,3‡], Bongibethu M. Hlabano-Moyo[2], Shanganyane P. Hlangothi[1]

[1]Department of Chemistry, Faculty of Science, Nelson Mandela University, Building 13, University Way, Gqeberha, 6011, South Africa

[2]Department of Civil, Construction and Environmental Engineering, College of Engineering, Iowa State University, 137 Town Engineering Building, 813 Bissel Rd, Ames, IA 50011-1066, USA

[3]Department of Applied Chemistry, Faculty of Applied Sciences, National University of Science and Technology, Chemistry Building, Gwanda Rd, Bulawayo, Zimbabwe

(s215391977@mandela.ac.za, bhlabano@iastate.edu, percy.hlangothi@mandela.ac.za)

‡ Corresponding Author; Bothwell Nyoni, Building 13, University Way, Gqeberha, 6011, South Africa, Tel: +27 63 436 7594, Fax: +27 41 504 4236, s215391977@mandela.ac.za

Received: 04.07.2022 Accepted: 05.08.2022

Abstract- A study of the pyrolysis of *Spirulina* and *Scenedesmus* microalgae in a rotary kiln is presented in this work. Thermogravimetric analysis of the two types of microalgae was performed prior to the actual pyrolysis in a bench scale rotary kiln that was equipped with a vapor condensation system. Thermogravimetric analysis revealed that the pyrolysis process of the two microalgae reaches peak reactivity at 335 – 345 ^{o}C. The bio-oils synthesized using the rotary kiln contained citronellyl iso-valerate (23.71 %) and phytol (13.49 %) for *Scenedesmus* and citronellyl iso-valerate (11.26 %), palmitic acid (10.7 %), phytol (7.07 %) and decanamide (6.11 %) for *Spirulina*. Furthermore, the proportion of compound classes in bio-oil was dominated by fatty acids, fatty acid esters and alcohols in the proportions 8.38, 31.3, 21.45 % and 15.38, 14.74, 16.18 % for *Scenedesmus* and *Spirulina*, respectively. However, detrimental nitrogen and sulfur containing heterocyclic compounds were found to be present in bio-oil. Results from this work suggest that algal biomass is a promising feedstock for bio-oil synthesis provided that the available downstream processes can reduce the nitrogen and sulfur containing compounds.

Keywords Algal biomass, Bio-oil, Rotary kiln, *Scenedesmus*, *Spirulina*

1. Introduction

Biomass has the potential of contributing significantly to sustainable energy especially in transportation fuels [1–3]. Biomass is classified into edible plants, non-edible plants, algae and modified organisms. Unlike woody biomass, algal biomass is composed of proteins (long chain amino acids), carbohydrates (sugars) and lipids (fats and oils). The use of algal biomass as an energy source looks promising, however, studies of large-scale production by use of photo-bioreactors and energy conversion technologies such as liquefaction, gasification and pyrolysis are necessary in order to position algal biomass as a potentially viable energy source [4, 5]. A recent study managed to show that biomass and hydro-power have the lowest installation capital costs (0.06 $/kWh) compared to concentrated solar power (0.22 $/kWh) [6]. Algal biomasses that have potential of large-scale cultivation are classified into cyanobacteria and chlorophyceae (green algae). *Spirulina* (cyanobacteria) and *Scenedesmus* (chlorophyceae) microalga have protein contents of 46 – 63 and 50 – 56 % respectively [7, 8]. *Spirulina* is a blue-green alga, spiral shaped, multi-cellular and photosynthetic

bacterium that normally exists as filaments of approximately 0.5 mm in length. On the other hand, *Scenedesmus* is a green fresh-water algae, unicellular in nature with a diameter of approximately 5 – 10 µm and normally exist as 4-celled colonies [7]. Generally, *Scenedesmus* has higher carbohydrates and lipids content compared to *Spirulina*, which makes it more suitable as an energy source instead of it being a food source.

In order to efficiently use algal biomass in large scale pyrolysis equipment, it is important to first understand pyrolysis aspects such as the change in behaviour with temperature and heating rates, product distributions, process kinetics and energetics. These aspects are also useful in the design of other energy conversion processes such as liquefaction, gasification and combustion [9]. Depending on achievable solid heating rates and vapour residence times, reactors operate in different pyrolysis regimes. Furthermore, researchers have managed to prove that operating at intermediate to flash pyrolysis regimes has the capability of achieving improved yields of either the liquid or gas product [10–13]. Use of fast pyrolysis reactors such as fluidised bed reactors is associated with several challenges such as clogging of material and the ingress of char particles into the oil product [11]. Interestingly, the problems of clogging and solid contamination of oil can be avoided by use of intermediate pyrolysis reactors [11]. Rotary kilns and screw conveyors are common heating equipment that can be used as intermediate pyrolysis reactors [11].

This study is particularly focused on the comparison of the pyrolysis processes of *Spirulina* and *Scenedesmus* microalga, with specific focus on the chemical composition of the synthesised bio-oil. The specific objectives of this work are as follows; (1) understand the pyrolysis of *Spirulina* and *Scenedesmus* microalga by use of a thermogravimetric analysis (TGA) instrument, (2) use the information obtained to operate a bench-scale rotary kiln pyrolyser and (3) compare the bio-oil products' chemical composition. Numerous studies focusing on the pyrolysis of biomass have employed pyrolysis-gas chromatography-mass spectrometry (Py-GCMS) and other suitable instruments [14–18]. The major drawback with the use of such instruments is that the conditions used may not emulate the real conditions in industrial continuous pyrolysis reactors. Firstly, a Py-GCMS instrument emulates the action of a fixed-bed pyrolysis system instead of the state-of-the art continuous reactors that have the capability of attaining intermediate to fast heating rates. Secondly, Py-GCMS instrument is commonly used to analyse the compounds that are formed when a solid material undergoes thermal breakdown, these compounds are not necessarily the ones that will be obtained in a real-life pyrolysis system that is equipped with a vapour condensation system. This argument is supported by the work of Sotoudehniakarani et al. [18]. In their work, the pyrolysis of *Chlorella vulgaris* microalgae was studied by use of a Py-GCMS instrument and an Auger reactor of dimensions 5 and 90 cm diameter and length, respectively. The Auger reactor was operated at temperatures of 450 – 550 °C at a throughput of 0.5 kg/h and solid residence time of approximately 6.4 s. Bio-oil was obtained via a vapor condensation system and further prepared for GCMS analysis. The reported bio-oil yield was 47.7 % at a temperature of 550 °C. Interestingly, analysis via Py-GCMS revealed that the volatile compounds formed during pyrolysis at 550 °C were dominated by palmitic acid, linoleic acid, coniferyl alcohol, indolizine and 2-methyl phenol. On the other hand, the bio-oil obtained in the Auger reactor through condensation of the vapours had palmitic acid, 1-tetradecene, 3-nonadecene, 4-cyclopropyl-1-butene and indole as the major compounds. Hu et al. [19] used a fixed bed reactor that was equipped with a water cooled condenser to synthesise bio-oil from the pyrolysis of blue-green algae blooms. The bio-oil synthesised contained palmitic acid, methylbenzene, 4-methyl phenol, n-heptadecane, hexadecanamide and indole as the major compounds. It is important to note that there is a wide range of pyrolysis units that can be used for pyrolysis studies and the rotary kiln is preferred for this study because of its simplicity in design and operation [12]. However, based on our literature search, there is limited literature on the study of pyrolysis of algal biomass using rotary kiln reactors.

2. Materials and methods

2.1. Materials and Analysis

Microalgae samples were obtained from Innoventon, Nelson Mandela University, Gqeberha (formerly Port Elizabeth), South Africa, where they are cultivated in large scale bioreactors. Dry algae powder was mixed with water and dried in an oven at 40 °C overnight in order to form crumbs. The resultant crumbs were crushed to obtain material of size 1.68 – 2.38 mm by passing the material through screens of mesh sizes 8 and 10. A CHNS elemental analyser (vario EL cube, Elementar) was used to carry out ultimate analysis. A muffle furnace was used to perform proximate analysis following the procedures outlined in ASTM methods [20–22]. Protein, carbohydrate and lipids content for microalgae samples was determined via the Kjeldahl, phenol-sulfuric methods and Soxhlet extract, respectively. Functional groups present in microalgae and char samples were determined via FTIR spectroscopy. The individual compounds in bio-oil were identified via GCMS analysis.

2.2. Thermogravimetric Analysis

Thermo-gravimetric (TG) analysis was performed via a simultaneous DSC-TGA instrument (SDT Q600). In the instrument, a sample was heated to 600 °C (heating rate, 100 °C/min) in a nitrogen atmosphere (flow, 80 ml/min). A heating rate of 100 °C/min was selected and the rationale behind this being that industrial continuous pyrolysis reactors operate at intermediate pyrolysis regimes with heating rates in the range of 100 – 300 °C/min [10, 11, 13]. Furthermore, earlier studies carried out on a similar experimental unit showed that the heating rate range varies from 100 – 800 °C/min depending on reactor's rotary speed, set temperature and particle size [12]. The mass-loss data generated by the TGA instrument was processed using a commercial software package (Universal Analysis 2000, TA Instruments).

2.3. Rotary Kiln Pyrolysis

The setup (shown in Fig. 1) is composed of feed hopper, reactor pipe, furnace and ancillaries as labelled therein. The details of the reactor pipe, heating furnace, and ancillaries are given in previous work [12]. The rotational speed was maintained at 36 rpm thereby achieving solids residence times of an average of 0.8 min. The reactor set temperature was maintained at 400 °C. 50 g of microalgae sample was placed into the feed hopper and the system was purged by passing nitrogen through the reactor at a flow of 1 l/min for at least 30 s. As the rotary action of the hopper screw feeder and reactor was initiated, the material underwent pyrolysis as it moved down the reactor pipe's heated zone. Nitrogen gas was fed at a rate of 5 l/min at the discharge end of the reactor pipe in order to create an inert environment and help push the vapors formed into the condensation system. Furthermore, a nitrogen gas flowrate of 5 l/min helped maintain a vapor residence time of approximately 2.3 s (calculated) in the heated zone, typical for intermediate pyrolysis processes [11]. The pyrolysis vapors were bubbled through liquid nitrogen in order to condense the bio-oil products. The char exiting the reactor was dropped into a quench pot that was maintained at low temperatures by use of liquid nitrogen.

2.4. Bio-oil Analysis

During pyrolysis, the vapors formed were bubbled through liquid nitrogen. The liquid nitrogen was then allowed to evaporate leaving the pyrolysis liquid product behind. 200 ml of dichloromethane (DCM) solvent was added and allowed to settle for 12 hours. The bottom oily layer (bio-oil) was decanted and concentrated via a rotary evaporator under reduced pressure before being sent for GCMS and FTIR analysis. The spectrums were obtained from an FTIR (Tensor 27, Bruker, USA) spectrometer, equipped with a broadband KBR beam splitter. The samples were scanned between the wavelengths of 400 – 4000 cm-1 at a resolution of 4 cm-1 with 50 scans. The spectra data generated was analysed using OPUSTM software (full GLP and 21 CFR part 11 compliant). The compounds were identified by means of a GCMS instrument; Agilent 7890A/5975C/7693 GC/Mass Spectrometer/Autosampler system (Agilent Technologies, USA). A fused silica capillary column SLB-5ms (Supelco, Sigma-Aldrich, USA) of dimensions 30 m length, 0.25 mm dimeter and 0.25 µm film thickness, was used. The carrier gas used was helium set at a flowrate of 1.8 ml/min and injection port temperature of 250 °C. The heating program was set as follows: hold for 2 min at 50 °C, heat to 300 °C at a heating rate of 10 °C/min and hold for 4 min, with a total run time of 31 min. At the GC inlet, the samples were injected at a split ratio of 20:1. The MS was operated in full-scan mode, scan range of m/z 45 – 600, with electron ionization voltage set at 70 eV, respectively. The eluted compounds were identified using NIST 2017 library matching. The mass spectra data and GC-total ion chromatography (TIC) profiles were generated using a commercial software (GC/MSD Productivity ChemStation, Agilent Technologies). HPLC grade DCM was used as solvent in all analyses. Graphical presentations of data points obtained from FTIR and GCMS software were prepared using MS-Excel.

3. Results and Discussion

3.1. Proximate and Ultimate Analysis

The proximate, ultimate and biochemical analyses of *Spirulina* and *Scenedesmus* algae are presented in Table 1. There is no clear-cut difference between the moisture and volatile content for the two algae types, however, *Spirulina* displays high ash and a lower fixed carbon content. Furthermore, since *Spirulina* is a cyanobacteria, its protein content, as expected, is higher than that of *Scenedesmus*. It is clear that the two algae types have high volatile matter which makes them suitable as feedstocks for the synthesis of bio-oil through pyrolysis and other liquefaction processes. Like most biomass, both algae have a considerably high oxygen/carbon molar ratio indicating a huge presence of polar compounds that manifest as phenols and other oxygenated compounds in the resultant pyrolysis oil. On comparison of the two algae types, *Spirulina* has a higher oxygen/carbon molar ratio. Most polar constituents in bio-oils, for example, phenols, tend to re-polymerise and form solid fragments thereby making the oil unsuitable for use [23]. This is expected to be a major drawback associated with the use of liquid fuels synthesised from pyrolysis of biomass. The hydrogen/carbon ratio of the two algae types is considerably high compared to other biomass, for example, compared to that of pine wood (1.55) presented by Wang et al. [24]. The hydrogen/carbon ratio is an indicator of the yield of oil that is expected when biomass undergoes pyrolysis process. The higher hydrogen/carbon ratio of the two algae indicates higher pyrolysis oil yield. Furthermore, studies have shown that the content of aromatic and unsaturated hydrocarbons in the resultant pyrolysis oil increases with increasing hydrogen/carbon ratio [24, 25]. The nitrogen/carbon ratio of the two algae types is high compared to other biomass materials and coal. This is due to protein in algae, whose basic structural units are mainly amino acids. Nyoni et al. [26] presented a comparison of the three materials where it was reported that the nitrogen/carbon ratios of algae, pinewood and coal were 0.2, 0.07 and 0.02. The generally high nitrogen/carbon ratio of algae can result in pyrolysis oil that has a high nitrogen content in the form of nitrogen based heterocyclic compounds such as azoles, pyrroles and pyridines. It is clear that *Spirulina* has a higher nitrogen/carbon ratio than *Scenedesmus*, this can be attributed to *Spirulina* higher protein content.

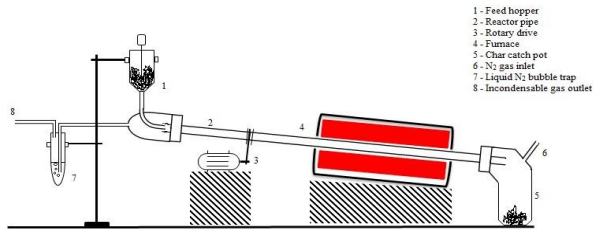

Fig. 1. Rotary kiln pyrolysis setup

Table 1. Analyses of *Spirulina* and *Scenedesmus* algae

	Spirulina	***Scenedesmus***
Ultimate analysis (wt		
Carbon	37.2	45.6
Hydrogen	4.9	6.6
Nitrogen	17.6	11.1
Sulfur	0.1	0.5
Oxygen	40.2	36.2
Proximate analysis (wt		
Moisture	6.3	7.6
Volatiles	67.4	67.8
Ash	16.5	11.1
Fixed carbon	9.8	13.5
Biochemical analysis		
Protein	60.3	48.5
Carbohydrates	10.9	18.3
Lipids	6.2	14.5
Oxygen/Carbon ratio	0.8	0.6
Hydrogen/Carbon ratio	1.6	1.7
Nitrogen/Carbon ratio	0.4	0.2

**dry, ash free basis*

3.2. Thermogravimetric Analysis

Fig. 2 shows mass-loss (TG) and derivative mass-loss plots (DTG) for the pyrolysis of the two algae types at a heating rate of 100 °C/min. From the TG curves, it is clear that the pyrolysis process is almost completed at a temperature of 600 °C. From the DTG curves, it can be deduced that the pyrolysis process reaches a peak at a temperature range of approximately 335 – 345 °C. The height of the DTG curves are a direct measure of the speed of the overall pyrolysis reaction, referred to as instantaneous reactivity in other works [27–28]. The difference in the heights of the curves implies that there is a difference between the speed of the main pyrolysis reactions between the two algae. This can be attributed to the differences in cell structure or biochemical composition. It is known that in slow or conventional pyrolysis of algae, proteins decompose first, followed by carbohydrates and then lastly, lipids [28–30]. However, at increased heating rates, these constituents may decompose simultaneously. This is represented by the sharp peak of the DTG curve, the shoulders appearing on the right-hand side of the peaks correspond to the decomposition of lipids. However, the shoulder for *Scenedesmus* DTG is more pronounced, confirmation that *Scenedesmus* contains a significant amount of lipids as compared to *Spirulina*. From this TGA analysis, it can be deduced that the reactor should be operated at a temperature that will result in the material being pyrolyzed at a temperature of approximately 335 – 345 °C, such as a reactor set temperature of 400 °C.

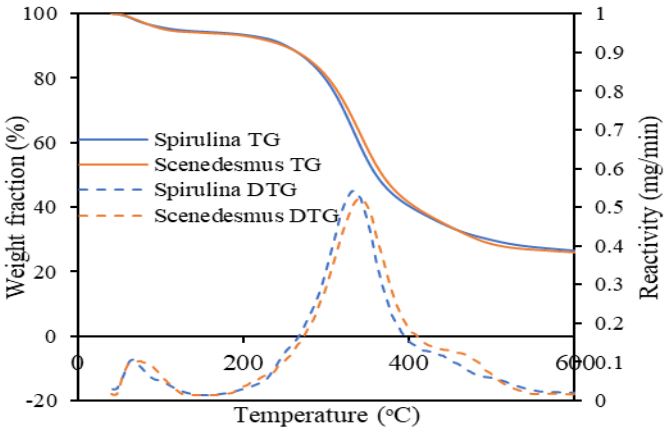

Fig. 2. TG and DTG plots for pyrolysis of *Spirulina* and *Scenedesmus* algae [Heating rate, 100 °C/min, 80 ml/min N_2 flow]

3.3. FTIR Spectroscopy Analysis

The FTIR spectrums of the two algae samples and their resultant chars are given in Fig. 3. The bands that appear in the spectra are characteristic of algal biomass. The broad band appearing at approximately 3000 – 3600 cm^{-1} corresponds to –OH and –NH groups of alcohols and moisture, and amines, respectively. The peak at 2920 cm^{-1} corresponds to the C–H bond stretching vibrations of the methyl and other alkyl groups [31–32]. The sharp peak at approximately 1640 cm^{-1} corresponds to the C=C bond stretching of monosubstituted alkenes. The peak at 1530 cm^{-1} for *Scenedesmus* is assignable to N–O stretching of the nitro compounds, whilst the peak at 1490 cm^{-1} for *Spirulina* corresponds to C–H bending vibrations of alkanes [33]. O–H bond bending vibrations due to carboxylic acids appear as weak peaks at approximately 1410 cm^{-1}. The peak at 1240 cm^{-1} corresponds to the C–O bond stretching vibrations of alkyl aryl ethers in carbohydrates or esters in lipids. Organic, inorganic acid anhydrides and sulfoxides appear as CO–O–CO and S=O bonds stretching vibrations in the range 1030 – 1070 cm^{-1}. Lastly, the peaks appearing in the range 400 – 800 cm^{-1} correspond to the C–I, C–Br and C–Cl bonds stretching of halogenated organic compounds found in algae. Majority of the peaks between *Scenedesmus* and *Spirulina* have the same wavenumbers, however, the peaks for *Spirulina* are lower. There are several factors that can be attributed to this observation. Firstly, the concentration of the compounds with the identified functional groups might be lower on *Spirulina*. Secondly, due to the morphology of the surface of the *Spirulina* sample, some intensity of the IR beam is lost during analysis. Thirdly, the existence of significant amounts of heavy metals such as Ni, Zn, Pb and Hg, particularly in majority of biomass samples causes

interactions that influence the height of spectra [34–36]. It is clear from the spectra that the char samples do not show the majority of peaks that have been mentioned. This implies that most of the compounds that contained the detected functional groups got decomposed during the pyrolysis process. However, *Scenedesmus* char displays weak peaks at 550 and 1100 cm^{-1} that correspond to the C–Cl and C–O bond stretching vibrations of chlorinated organic compounds and tertiary alcohols, respectively. These are higher boiling point compounds that offer significant resistance to thermal decomposition and release from the crystalline matrix of the algae material. Higher temperatures and slower heating rates may be required in order to decompose chlorinated organic compounds and tertiary alcohols contained within algae.

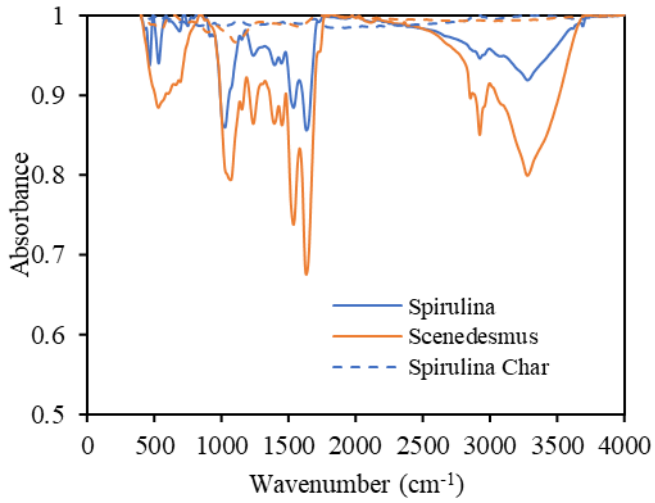

Fig. 3. FTIR spectra for *Spirulina* and *Scenedesmus* algae before and after pyrolysis in a rotary kiln pyrolyser

3.4. Bio-oil Composition Analysis

Fig. 4 shows the GC-TIC of bio-oil synthesised from the pyrolysis of *Spirulina* and *Scenedesmus* in a rotary reactor. From the number of peaks that appear, it is clear that the bio-oil is a complex liquid that contains a large number of compounds. The major compounds (those with ≥ 1.0 % of the total area) are labelled (1 – 33) and listed in Table 2. The most abundant compounds in *Scenedesmus* bio-oil are citronellyl iso-valerate (peak no. 14) and phytol (peak no. 16), with proportions of 23.71 and 13.49 %, respectively. *Spirulina* bio-oil displays four abundant compounds, namely citronellyl iso-valerate (peak no. 14), palmitic acid (peak no. 19), phytol (peak no. 16) and decanamide (peak no. 21), in the proportions 11.26, 10.7, 7.07 and 6.11 %, respectively. Citronellyl iso-valerate, is a fatty acid ester and fatty acid esters are major components of biodiesel derived from vegetable and animal fat. Biodiesels have the advantage of low exhaust emissions whem used in a conventional diesel engine [37]. However, there is not much literature that covers the use of citronellyl iso-valerate in general. Phytol is a diterpene alcohol which is released in the thermal decomposition of chlorophyl [38]. A recent study has shown that phytol can be subjected to catalytic cracking to produce gasoline with a high-octane number [39]. Palmitic acid (hexadecenoic acid) is a saturated fatty acid. In the synthesis of biodiesel, fatty acids esters are synthesised by the transesterification of fatty acids in vegetable and animal fat. Decanamide is a fatty amide derived from decanoic acid.

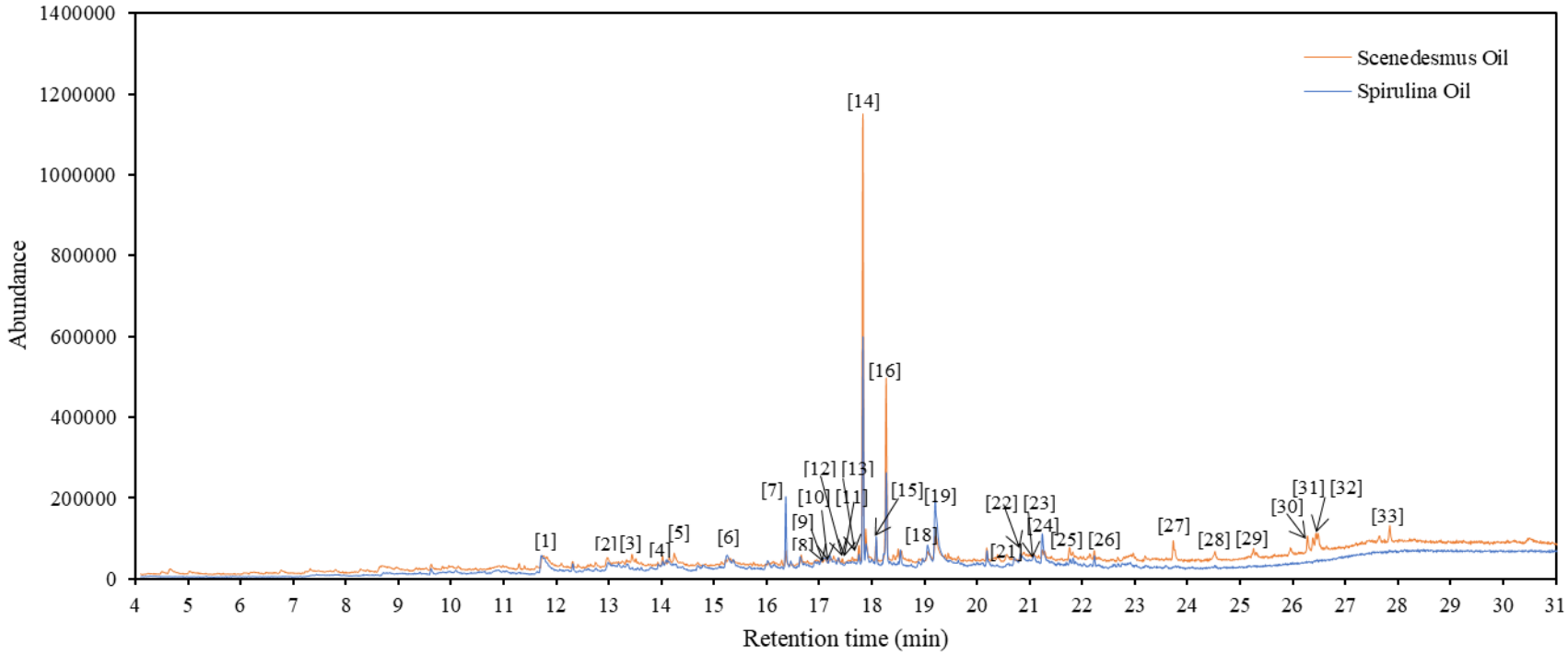

Fig. 4. GC-TIC of bio-oil synthesised from the pyrolysis of *Spirulina* and *Scenedesmus* algae in a rotary kiln pyrolyser

In order to enable a comparison of physical properties with pyrolysis oils synthesised elsewhere and commercial fuels, columns of molecular weights and gross calorific values (GCV) are included in Table 2. GCV can be calculated if atomic ratio is known [41–44] The molecular weights are seen to be in the range of 128 – 423 g/mol which is not in agreement with the works of Sotoudehniakarani et al. [18] and Hu et al. [19]. Sotoudehniakarani et al. [18] reported oil with compounds will molecular weights in the range 56 – 322 g/mol. These differences can be attributed to the different algae types used. Furthermore, the solvents used and sample preparation methods prior to GC-MS analysis were different. The GCV of compounds presented in Table 2 varies from 10.19 to 48.36 MJ/kg with halogenated aromatic or cyclic compounds having the lowest GCV. The presence of halogenated compounds has a detrimental effect on the energy content of the oil synthesised from algal biomass pyrolysis. Therefore, techniques of reducing the halogenated compounds content must be explored. The calculated average GCV for bio-oils in this study turns out to be 27.4 and 29.6 MJ/kg for *Spirulina* and *Scenedesmus* respectively. These values are in good agreement with the works of Bordoloi et al. [43] who reported a GCV of 28.5 MJ/kg for bio-oil synthesised from the pyrolysis of *Scenedesmus*. However, Zhou and Hu [45] managed to show that the hydrothermal liquefaction of algal biomass gives bio-oil of higher GCV. Generally, the GCV of bio-oils is lower than that of commercial petroleum-based ones but can be upgraded.

Upon grouping the compounds in Table 2 into classes, namely, halogenated aromatics, nitrogen containing polycyclic aromatic hydrocarbons (PANH), organosulfur, heterocycles (nitrogen containing), oxygenated aromatics, paraffins, cyclic ketones, unsaturated aliphatics, fatty acid esters, alcohols, nitriles, fatty acid, amides and cyclic hydrocarbons, the resultant proportions are shown in Fig. 5. It is clear that the composition of the two algae is dominated by fatty acids, fatty acid esters and alcohols. However, on comparison, bio-oil from *Scenedesmus* displays a significantly large amount of fatty acid esters. On the other hand, bio-oil from *Spirulina* has a higher proportion of fatty acids. This observation can be attributed to the generation of fatty acid esters from esterification reactions between alcohols and fatty acids taking place within the pyrolysis vapours. The two bio-oils display considerable amounts of compounds that have the capability of improving the fuel properties. These compounds are paraffins, cyclic ketones and unsaturated aliphatics. Ketones are produced via the hydrolysis and dehydration of polysaccharides and cellulose [19]. Unsaturated aliphatics are generated from the breakdown of unsaturated fatty acids found in lipids. The presence of nitrogen and sulfur containing compound groups is detrimental because they contribute to NO_x and SO_x emissions. There is a general consensus between this study and the works of Lopez-Aguilar et al. [17] where a Py-GCMS instrument was used. Nitrogen containing compounds were found to dominate the composition of volatile compounds. Hu et al. [19] used a fixed bed reactor for pyrolysis of blue-green algae. There is good agreement with results presented in this work on the identity of the compounds constituting the bio-oil; palmitic acid was detected as the major compound. Sotoudehniakarani et al. [18] studies on pyrolysis of algae in an Auger reactor were the closest to this current study. As expected, palmitic acid was detected as the major compound in bio-oil; this is consistent with the results presented in this work. Interestingly, there is a huge difference in the composition of the oil synthesised in this study and that of Costa et al. [46] because the material used was lignocellulosic biomass. This observation is proof that oils synthesised from algal biomass have a different chemical composition compared to those obtained from woody biomass. A detailed comparative pyrolysis study of lentil husk and algae was recently presented by Targhi et al. [47] where it was revealed that algae oil contained a significantly large proportion of alcohols and nitrogen containing compounds.

4. Conclusion

This study performed a comparison of the pyrolysis of two common types of algae, i.e., *Spirulina* and *Scenedesmus* microalgae, with specific focus on the synthesised bio-oils. This was achieved by employing a rotary kiln pyrolyser that operates at intermediate pyrolysis regimes. Results showed that the most abundant compounds in *Scenedesmus* bio-oil were citronellyl iso-valerate. *Spirulina* bio-oil contained four major compounds, namely citronellyl iso-valerate, palmitic acid, phytol and decanamide. In terms of classes of compounds, the composition of the two algae bio-oils is dominated by fatty acids, fatty acid esters and alcohols. However, nitrogen and sulfur containing heterocycles were also detected in the bio-oils. From this study, there is a strong indication that pyrolysis processes of microalgae in intermediate pyrolysis reactors such as rotary kilns have the potential of being one of the major routes in the synthesis of renewable liquid fuels.

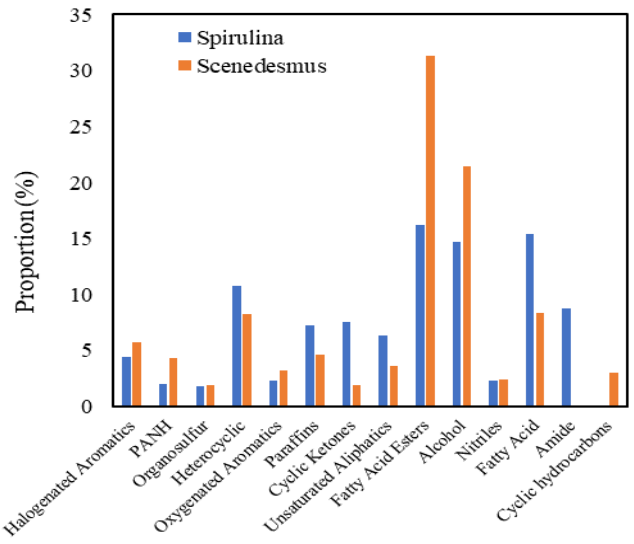

Fig. 5. Proportion of compound classes in bio-oil synthesised from the pyrolysis of *Spirulina* and *Scenedesmus* algae in a rotary kiln pyrolyser

Table 2. Main compounds of *Spirulina* and *Scenedesmus* bio-oil as identified by GCMS analysis

No.	RT (min)	Compound name	Molecular formula	MW (g/mol)	GCV* (MJ/kg)	Area (%)		Compound class
						Spirulina	*Scenedesmus*	
1	11.777	Benzene, 1,2,3,5-tetrachloro-4,6-difluoro-	$C_6Cl_4F_2$	252	10.19	3.10	2.01	Halogenated aromatics
2	13.036	1H-Indole, 2-methyl-	C_9H_9N	131	38.34	1.42	1.61	PANH
3	13.414	Cyclopropane carboxylic acid-2-pentyl, ethyl(-2-butylthio) ester	$C_{15}H_{28}O_2S$	272	36.11	-	1.44	Organosulfur
4	14.100	4-Phenyl-1,2,3,6-tetrahydropyridine	$C_{11}H_{13}N$	159	40.01	-	1.00	Heterocyclic
5	14.215	Benzene, 1-methyl-3-phenoxy-	$C_{14}H_{14}O$	198	38.33	-	1.21	Oxygenated aromatics
6	15.216	N-[6-[N-Aziridyl]-3-aza-3-hexenyl] morpholine	$C_{11}H_{21}N_3O$	211	33.32	2.72	-	Heterocyclic
7	16.326	Cyclohexane, undecyl-	$C_{17}H_{34}$	238	47.83	4.02	1.13	Cyclic hydrocarbon
8	16.624	Heptadecane	$C_{17}H_{36}$	240	48.36	1.05	1.27	Paraffin
9	17.036	4-Fluorothiophenol	C_6H_5FS	128	28.55	1.26	-	Organosulfur
10	17.064	Piperazine, 1,2,4-trimethyl-	$C_7H_{16}N_2$	128	38.36	1.42	-	Heterocyclic
11	17.167	Ethanone, 1-(2,2-dimethylcyclopentyl)-	$C_9H_{16}O$	140	39.86	1.57	-	Cyclic ketone
12	17.322	1,4-Benzenediol, 2,3,5-trimethyl-	$C_9H_{12}O_2$	152	32.31	1.64	1.22	Oxygenated aromatics
13	17.717	Phytene-2	$C_{20}H_{40}$	280	47.83	1.10	1.50	Unsaturated Aliphatic
14	17.791	Citronellyl iso-valerate	$C_{15}H_{28}O_2$	240	39.06	11.26	23.71	Fatty acid ester
15	18.043	Citronellol	$C_{10}H_{20}O$	156	41.49	1.94	1.67	Alcohol
16	18.232	Phytol	$C_{20}H_{40}O$	296	44.49	7.07	13.49	Alcohol
17	18.501	Hexadecanenitrile	$C_{16}H_{31}N$	237	44.73	1.59	1.82	Nitrile
18	19.021	L-Proline, N-valeryl-, hexadecyl ester	$C_{26}H_{49}NO_3$	423	38.78	3.34	2.26	Heterocyclic
19	19.170	Palmitic acid	$C_{16}H_{32}O_2$	256	40.11	10.70	6.35	Fatty acid
20	20. 143	Cyclohexane ethanol, 3-hydroxy-beta.,4-dimethyl-	$C_{10}H_{20}O_2$	172	36.33	1.25	1.09	Alcohol
21	20.778	7-Pentadecyne	$C_{15}H_{28}$	208	47.22	3.33	-	Unsaturated Aliphatic
22	20.938	9-Cycloheptadecen-1-one, (Z)-	$C_{17}H_{30}O$	250	42.85	1.16	1.41	Cyclic ketone
23	21.030	Cycloheptadecanone	$C_{17}H_{32}O$	252	43.40	2.54	-	Cyclic ketone
24	21.196	Decanamide	$C_{10}H_{21}NO$	171	38.51	6.11	-	Amide
25	21.711	Cyclooctadecene	$C_{18}H_{34}$	250	47.32	-	1.17	Cyclic hydrocarbon
26	21.773	9H-Fluorene, 2,3-dimethyl-	$C_{15}H_{14}$	194	42.57	-	1.10	Polycyclic hydrocarbon
27	23.679	1-Octadecene	$C_{18}H_{36}$	252	47.83	-	1.25	Unsaturated Aliphatic
28	25.201	Eicosane	$C_{20}H_{42}$	282	48.28	-	1.07	Paraffin
29	26.225	Ethyl 2-(2,2-dichlorovinyl)-3,3-dimethylcyclopropanecarboxylate	$C_{10}H_{14}Cl_2O_2$	237	23.43	-	1.49	Halogenated cyclic
30	26.328	Permethrine	$C_{21}H_{20}Cl_2O_3$	391	27.90	-	1.12	Halogenated aromatics
31	26.385	5-Acetamido-4,7-dioxo-4,7-dihydrobenzofurazan	$C_8H_5N_3O_4$	207	15.63	-	1.50	Heterocyclic
32	26.425	Propionaldehyde, (O-pentafluorobenzyl) oxime, (Z) or (E)-	$C_{10}H_8F_5NO$	253	19.74	-	1.21	Halogenated aromatics
33	27.782	Benzo[h]quinoline, 2,4-dimethyl-	$C_{15}H_{13}N$	207	39.36	-	1.65	PANH

**GCV calculated via empirical formulae given in literature* [40–42]

References

[1] R. P. John, G. S. Anisha, K. M. Nampoothiri, and A. Pandey, "Micro and macroalgal biomass: A renewable source for bioethanol", *Bioresour. Technol*, vol. 102, pp. 186–193, 2011. DOI: https://10.1016/j.biortech.2010.06.139.

[2] M. M. Wright, D. E. Daugaard, J. A. Satrio, and R. C. Brown, "Techno-economic analysis of biomass fast pyrolysis to transportation fuels", *Fuel*, vol. 89, pp. S2–S10, 2010. DOI: https://10.1016/j.fuel.2010.07.029.

[3] M. E. Shayan, G. Najafi, and A. Nazari, "The biomass supply chain network auto-regressive moving average algorithm", *Int. J. Smart Grid*, vol. 5, pp. 15–22, 2021. DOI: https://10.20508/ijsmartgrid.v5i1.153.g135.

[4] A. Demirbas, "Use of algae as biofuel sources", *Energy Convers. Manage*, vol. 51, pp. 2738–2749, 2010. DOI: https://10.1016/j.enconman.2010.06.010.

[5] P. McKendry, "Energy production from biomass (part 1): overview of biomass", *Bioresour. Technol*, vol. 83, pp. 37–46, 2002. DOI: https://10.1016/S0960-8524(01)00118-3.

[6] K. E. Okedu, aand M. Al-Hashmi, "Assessment of the cost of various renewable energy systems to provide power for a small community: Case of Bukha, Oman", *Int. J. Renew. Smart Grid*, vol. 3, pp. 173–182, 2018. DOI: https://10.20508/ijsmartgrid.v2i3.17.g179.

[7] E. W. Becker, "Micro-algae as a source of protein", *Biotechnol. Advances*, vol. 25, pp. 207–210, 2007. DOI: https://10.1016/j.biotechadv.2006.11.002.

[8] M. A. Toyub, M. I. Miah, M. A. B. Habib, and M. M. Rahman, "Growth performance and nutritional value of *Scenedesmus obliquos* cultured in different concentrations of sweetmeat factory waste media", *Bangladesh J. Anim. Sci*, vol. 37, pp. 86–93, 2008. DOI: https://10.3329/bjas.v37i1.9874.

[9] A. I. Mabuda, N. S. Mamphweli, and E. L. Meyer, "Model free kinetic analysis of biomass/sorbent blends for gasification purposes", *Renew. Sustain. Energy Rev*, vol. 53, pp. 1656–1664, 2016. DOI: https://10.1016/j.rser.2015.07.038.

[10] A. V. Bridgwater, P. Carson, and M. Coulson, "A comparison of fast and slow pyrolysis liquids from mallee", *Int. J. Glob. Energy Issues*, vol. 27, pp. 204–216, 2007. DOI: https://10.1504/IJGEI.2007.013655.

[11] A. Hornung, "Intermediate pyrolysis of biomass", In: Rosendahl L, editors. *Biomass Combustion Science, Technology and Engineering*, Birmingham: Woodhead, 2013, pp. 172–186.

[12] Nyoni B., and Hlangothi S., "Evaluation of the thermal decomposition behaviour of algal biomass in a rotary kiln pyrolyser", *2021 9th International Renewable and Sustainable Energy Conference (IRSEC)*, Morocco, pp. 1–4, 23–27 November 2021. DOI: https://10.1109/IRSEC53969.2021.9741174.

[13] Y. Yang, J. G. Brammer, A. S. N. Mahmood, and A. Hornung, "Intermediate pyrolysis of biomass energy pellets for producing sustainable liquid, gaseous and solid fuels", *Bioresour. Technol*, vol. 169, pp. 794–799, 2014. DOI: https://10.1016/j.biortech.2014.07.044.

[14] R. R. Dirgarini, J. N. Subagyono, Y. Qi, W. R. Jackson, and A. L. Chaffee, "Pyrolysis-GC/MS analysis of biomass and the bio-oils produced from CO/H_2O reactions", *J. Anal. Appl. Pyrolysis*, vol. 120, pp. 154–164, 2016. DOI: https://10.1016/j.jaap.2016.05.001.

[15] G. Bensidhom, M. Arabiourrutia, A. B. H. Trabelsi, M. Cortaza, S. Ceylan, and M. Orlaza, "Fast pyrolysis of date palm biomass using Py-GCMS", *J. Energy Institute*, vol. 99, pp. 229–239, 2021. DOI: https://10.1016/j.joei.2021.09.012.

[16] Z. Wang, Y. Che, J. Li, W. Wu, B. Yan, Y. Zhang, X. Wang, F. Yu, G. Chen, X. Zuo, and X. Li, "Effects of anaerobic digestion pretreatment on the pyrolysis of *Sargassum*: Investigation by TG-FTIR and Py-GC/MS", *Energy Convers. Manage*, vol. 267, pp. 1–9, 2022. DOI: https://10.1016/j.enconman.2022.115934.

[17] H. A. Lopez-Aguilar, D. Quiroz-Cardoza, and A. Perez-Hernandez, "Volatile compounds of algal biomass pyrolysis", *J. Mar. Sci. Eng*, vol. 10, pp. 1–16, 2022. DOI: https://10.3390/jmse10070928.

[18] F. A. Sotoudehniakarani, A. Alayat, and A. G. McDonald, "Characterization and comparison of pyrolysis products from fast pyrolysis of commercial *Chlorella vulgaris* and cultivated microalgae", *J. Anal. Appl. Pyrolysis*, vol. 139, pp. 258–273, 2019. DOI: https://10.1016/j.jaap.2019.02.014.

[19] Z. Hu, Y. Zheng, F. Yan, B. Xiao, and S. Liu, "Bio-oil production through pyrolysis of blue-green algae blooms (BGAB): Product distribution and bio-oil characterization", *Energy*, vol. 52, pp. 119–125, 2013. DOI: https://10.1016/j.energy.2013.01.059.

[20] ASTM D3172-07a, Standard Practice for Proximate Analysis of Coal and Coke, *ASTM International*, 2007.

[21] ASTM E871, Standard Test Method for Moisture Analysis of Particulate Wood Fuels, *ASTM International*, 2013.

[22] ASTM E872, Standard Test Method for Volatile Matter in the Analysis of Particulate Wood Fuels, *ASTM International*, 2013.

[23] J. P. Diebold, and S. Czernik, "Additives to lower and stabilize the viscosity of pyrolysis oils during storage", *Energy Fuels*, vol. 11, pp. 1081–1091, 1997. DOI: https://10.1021/ef9700339.

[24] M. Wang, S. L. Zhang, and P. G. Duan, "Slow pyrolysis of biomass: effects of effective hydrogen-to-carbon atomic ratio of biomass and reaction atmospheres", *Energy Sources Part A*, vol. 42, pp. 1–14, 2019. DOI: https://10.1080/15567036.2019.1665150

[25] T. P. Vispute, H. Zhang, A. Sanna, R. Xiao, and G. W. Huber, "Renewable chemical comodity feedstocks from integrated catalytic processing of pyrolysis oils", *Sci*, vol. 330, pp. 1222–1227, 2010. DOI: https://10.1126/science.1194218.

[26] B. Nyoni, S. Duma, S. Shabangu, and S. Hlangothi, "Comparison of the slow pyrolysis behaviour and kinetics of coal, wood and algae at high heating rates", *Nat. Resour. Res*, vol. 29, pp. 3943–3955, 2020. DOI: https://10.1007/s11053-020-09687-3.

[27] K. Kirtania, and S. Bhattacharya, "Pyrolysis kinetics

and reactivity of algae-coal blends", *Biomass Bioenergy*, vol. 55, pp. 291–298, 2013. DOI: https://10.1007/s11053-020-09687-3.

[28] B. Nyoni, S. Duma, L. Bolo, S. Shabangu, and S. P. Hlangothi, "Co-pyrolysis of South African bituminous coal and Scenedesmus microalgae: Kinetics and synergistic effects study", *Int. J. Coal Sci. Technol*, vol. 7, pp. 807–815, 2020. DOI: https://10.1007/s40789-020-00310-7.

[29] Q. V. Bach, and W. H. Chen, "Pyrolysis characteristics and kinetics of microalgae via thermogravimetric analysis (TGA): State-of-the-art review", *Bioresour. Technol*, vol. 131, pp. 109–116, 2014. DOI: https://10.1016/j.biortech.2017.06.087.

[30] J. Wang, W. Lian, P. Li, Z. Zhang, J. Yang, X. Hao, W. Huang, and G. Guan, "Simulation of pyrolysis in low rank coal particle by using DAEM kinetics model: Reaction behavior and heat transfer", *Fuel*, vol. 207, pp. 126–135, 2017. DOI: https://10.1016/j.fuel.2017.06.078.

[31] T. A. Khan, A. A. Mukhlif, E. A. Khan, and D. K. Sharma, "Isotherm and kinetics modelling of Pb(II) and Cd(II) adsorptive uptake from aqueous solution by chemically modified green algal biomass", *Model Earth Syst. Environ*, vol. 117, pp. 1–13, 2016. DOI: https://10.1007/s40808-016-0157-z.

[32] N. Sebeia, M. Jabli, A. Ghith, Y. Elghoul, and F. M. Alminderej, "Production of cellulose from *Aegagrobia Linnaei* macro-algae: Chemical modification, characterization and application for the bio-sorption of cationic and anionic dyes from water", *Int. J. Biol. Macromolecules*, vol. 135, pp. 152–162, 2019. DOI: https://10.1016/j.ijbiomac.2019.05.128.

[33] L. S. Ferreira, M. S. Rodrigues, J. C. M. de Carvalho, A. Lodi, E. Finocchio, P. Perego, and A. Converti, "Adsorption of Ni^{2+}, Zn^{2+} and Pb^{2+} onto dry biomass of *Anthrospira (Spirulina) plantesis* and *Chlorella vulgaris.* I. Single metal systems", *Chem. Eng. J*, vol. 173, pp. 326–333, 2011. DOI: https://10.1016/j.cej.2011.07.039.

[34] N. A. Al-Dhabi, "Heavy metal analysis in commercial *Spirulina* products for human consumption", *Saudi J. Biol. Sci*, vol. 20, pp. 383–388, 2013. DOI: https://10.1016/j.sjbs.2013.04.006.

[35] M. Mamera, J. J. van Tol, M. P. Aghoghovwia, and E. Kotze, "Sensitivity and calibration of the FT-IR spectroscopy on concentration of heavy metal ions in river and borehole water sources", *Appl. Sci*, vol. 10, pp. 1–16, 2020. DOI: https://10.3390/app10217785.

[36] A. A. Yusuf, and F. L. Inambao, "Characterization of Ugandan biomass wastes as the potential candidates towards bioenergy production", *Renew. Energy Sustain. Rev*, vol. 117, pp. 1–10, 2020. DOI: https://10.1016/j.rser.2019.109477.

[37] Arslan, R., and Ulusoy, Y., "Utilisation of waste cooking oil as an alternative fuel for Turkey", *2015 5th International Conference on Renewable Energy Research and Applications (ICRERA)*, UK, pp. 728–731, 20–23 November 2015. DOI: https://10.1109/ICRERA.2016.7884526.

[38] S. Kraub, and W. Vetter, "Phytol and phytyl fatty acid esters: Occurrence, concentrations and relevance", *European J. Lipid Sci. Technol*, vol. 120, pp. 1–14, 2018. DOI: https://10.1002/ejlt.201700387.

[39] N. I. Tracy, D. W. Crunkleton, and G. L. Price, "Gasoline production from phytol", *Fuel*, vol. 89, pp. 3493–3497, 2010. DOI: https://10.1016/j.fuel.2010.06.022.

[40] A. Dirmibas, D. Gullu, A. Caglar, and F. Akdeniz, "Estimation of calorific values of fuel from lignocellulosics", *Energy Sources*, vol. 19, pp. 765–770, 1997. DOI: https://10.1080/00908319708908888.

[41] A. Dirmibas, N. Ak, A. Aslan, and N. Sen, "Calculation of higher heating values of hydrocarbon compounds and fatty acids", *Petroleum Sci. Technol*, vol. 36, pp. 712–717, 2018. DOI: https://10.1080/10916466.2018.1443126.

[42] Khalida B., Mohamed Z., Belaid S., Samir H. O., Sobhi K., and Midane S., "Prediction of higher heating value HHV of date palm biomass fuel using artificial intelligence method", *2019 8th International Conference on Renewable Energy Research and Applications (ICRERA)*, Romania, pp. 59–62, 03–06 November 2019. DOI: https:// 10.1109/ICRERA47325.2019.8997113.

[43] N. Bordoloi, R. Narzari, D. Sut, R. Saikia, R. S. Chutia, and R. Kataki, "Characterisation of bio-oil and its sub-fractions from pyrolysis of *Scenedesmus dimorphus*", *Renew. Energy*, vol. 98, pp. 245–253, 2016. DOI: https://10.1016/j.renene.2016.03.081.

[44] Hosokai, S., Matsuoka, K., Kuramoto, K., and Suzuki, Y., "Estimation of thermodynamic properties of liquid fuel from biomass pyrolysis", *2014 3rd International Conference on Renewable Energy Research and Applications (ICRERA)*, USA, pp. 728–731, 09–22 October 2014. DOI: https://10.1109/ICRERA.2014.7016481.

[45] Y. Zhou, and C. Hu, "Catalytic thermochemical conversion of algae and upgrading of algal oil for the production of high-grade liquid fuel: A review", *Catalysts*, vol. 10, pp 1–24, 2020. DOI: https://10.3390/catal10020145.

[46] P. A. Costa, M. A. Barreiros, A. I. Mouquinho, P. O. Silva, F. Paradela, and F. A. C. Oliveira, "Slow pyrolysis of cork granules under nitrogen atmosphere: by-products characterization and their potential valorization", *Biofuel Res. J*, vol. 33, pp. 1562–1572, 2022. DOI: https://10.18331/BRJ2022.9.1.3.

[47] N. K. Targhi, O. Tavakoli, and A.H. Nazemi, "Co-pyrolysis of lentil husk wastes and *Chlorella vulgaris*: Bio-oil and biochar yields optimization", *J. Anal. Appl. Pyrolysis*, vol. 165, pp. 1–16, 2022. DOI: https://10.1016/j.jaap.2022.105548.